Biomedicine & Pharmacotherapy 118 (2019) 109237

Contents lists available at ScienceDirect

Biomedicine & Pharmacotherapy

journal homepage: www.elsevier.com/locate/biopha

Oxidation derivative of (-)-epigallocatechin-3-gallate (EGCG) inhibits RANKL-induced osteoclastogenesis by suppressing RANK signaling pathways in RAW 264.7 cells

Huanhuan Xu[a,b,1], Titi Liu[a,c,1], Jin Li[a,c,1], Jing Xu[a,c], Fei Chen[a,c], Lihong Hu[a,c], Banglei Zhang[a,c], Chengting Zi[a,b,*], Xuanjun Wang[a,b,d,*], Jun Sheng[a,d,*]

[a] Key Laboratory of Pu-er Tea Science, Ministry of Education, Yunnan Agricultural University, Kunming, 650201, China
[b] College of Science, Yunnan Agricultural University, Kunming, 650201, China
[c] College of Food Science and Technology, Yunnan Agricultural University, Kunming, 650201, China
[d] State Key Laboratory for Conservation and Utilization of Bio-Resources in Yunnan, Kunming, 650201, China

ARTICLE INFO

Keywords:
EGCG
Oxidation derivative
Osteoclastogenesis
NFATc1
c-Fos
RANK signaling pathways

ABSTRACT

Tea consumption has positive effects on the skeletal system and prevents postmenopausal osteoporosis, mainly by inhibiting osteoclastogenesis. In green tea, (-)-epigallocatechin-3-gallate (EGCG) is the most abundant and active compound and has been shown to inhibit RANKL-induced osteoclast formation. Taking into account the highly oxidizable and unstable nature of EGCG, we hypothesized that EGCG oxidation product exhibits greater anti-osteoclastogenesis potential than EGCG. In this study, we successfully isolated and identified an EGCG oxidation derivative, (-)-gallocatechin gallate (compound **2**), using a chemical oxidation strategy. We then compared the ability of compound **2** and EGCG to inhibit RANKL-induced osteoclastogenesis in RAW 264.7 cells. The results of TRAP staining and F-actin ring immunofluorescent staining showed that compound **2** exhibits stronger inhibition of RANKL-induced osteoclast differentiation and F-actin ring formation, respectively, than EGCG. Additionally, quantitative real-time PCR (qRT-PCR) and western blotting analyses showed that compound **2** significantly and more strongly inhibited the expression of osteoclastogenesis-related marker genes and proteins, including c-Src, TRAP, cathepsin K, β3-Integrin, and MMP-9, compared with EGCG. Furthermore, compound **2** significantly suppressed RANKL-induced expression of NFATc1 and c-Fos, the master transcriptional regulators of osteoclastogenesis, more strongly than EGCG. Mechanistically, molecular interaction assays showed that compound **2** binds to RANK with high affinity (K_D = 189 nM) and blocks RANKL–RANK interactions, thereby suppressing RANKL-induced early RANK signaling pathways including p65, JNK, ERK, and p38 in osteoclast precursors. Taken together, this study demonstrates for the first time that an oxidation derivative of EGCG (compound **2**) inhibits RANKL-induced osteoclastogenesis by suppressing RANK signaling pathways in RAW 264.7 cells.

1. Introduction

Bone homeostasis is tightly regulated by the coupled action of osteoclasts that regulate bone resorption and osteoblasts that regulate bone formation via a process called remodeling [1]. An imbalance between the resorption of old bones and formation of new bones directly causes gross perturbations in the skeletal structure and function, potentially leading to morbidity and shortened lifespan [1,2]. Excess osteoclastic activity contributes to the development of many skeletal diseases, such as postmenopausal osteoporosis, rheumatoid arthritis, periodontal disease, multiple myeloma, and metastatic cancers [1,3]. Thus, inhibiting osteoclast differentiation and activation is a key therapeutic strategy for treating bone metabolic diseases [4].

Osteoclasts originate from hematopoietic stem cells and differentiate through monocyte and macrophage precursors to form mature osteoclasts, which are characterized by a clear zone, ruffled border, and the secretion of acid and lytic enzymes that degrade bone mineralized matrices [5,6]. The receptor activator of NF-κB (RANK) ligand (RANKL) plays an important role in osteoclastogenesis [7]. The binding of RANKL to its receptor RANK directly activates canonical RANK

* Corresponding authors at: Yunnan Agricultural University, Heilongtan, North of Kunming, Kunming, 650201, China.
E-mail addresses: zichengting@126.com (C. Zi), wangxuanjun@gmail.com (X. Wang), shengjunpuer@163.com (J. Sheng).
[1] These authors have contributed equally to this work.

https://doi.org/10.1016/j.biopha.2019.109237
Received 22 May 2019; Received in revised form 13 July 2019; Accepted 16 July 2019

signaling pathways during osteoclastogenesis, leading to the activation of many key transcription factors such as c-Fos and NFATc1 (short for Nuclear Factor of Activated T-Cells, Cytoplasmic1). These transcription factors regulate the expression of osteoclast-related marker genes such as tartrate-resistant acid phosphatase (TRAP), c-Src, cathepsin K, matrix metallopeptidase-9 (MMP-9), and c-Src, thus driving the formation and activation of mature osteoclasts [6,8,9].

Tea prepared from the green leaves of *Camellia sinensis* (L.) O. Kuntze is the second most consumed beverage worldwide, given its broad-spectrum beneficial effects on human health [10]. Tea is categorized into three types: green, black, and Pu-erh tea, depending on the processing technique [11]. Numerous studies have shown that tea consumption has positive effects on the skeletal system by effectively preventing and treating postmenopausal osteoporosis [12]. Catechins including (-)-epigallocatechin-3-gallate (EGCG), (-)-epicatechin-3-gallate (ECG), (-)-epigallocatechin (EGC), and (-)-epicatechin (EC) are the main active components of green tea and have diverse beneficial effects on human health [13]. Among these, EGCG has recently attracted great interest for its antiviral, anti-inflammatory, and anticancer properties [13–16]. Furthermore, EGCG has been shown to inhibit RANKL-induced osteoclast formation [17,18]. However, since EGCG is easily oxidized and is unstable at high pH or under prolonged exposure to high temperature [19,20], we hypothesized that oxidation products of EGCG would exhibit higher anti-osteoclastogenesis potential than EGCG.

In this study, we isolated and identified an EGCG oxidation derivative, (-)-gallocatechin gallate (GCG; compound **2**), using a chemical oxidation strategy. We tested the ability of compound **2** with EGCG to inhibit RANKL-induced osteoclast differentiation in RAW 264.7 cells. We also explored the potential molecular mechanisms underlying the inhibition of RANKL-induced osteoclast differentiation.

2. Materials and methods

2.1. Materials

High purity (> 98%) grade EGCG was purchased from Biopurify Phytochemicals Ltd. (Chengdu, China). High performance liquid chromatography (HPLC) grade methanol was obtained from J&K Chemical Technology Co., Ltd. (Beijing, China). All reagents were commercially available and used without further purification, unless indicated otherwise. All solvents were obtained from commercial sources and were purified according to standard procedures.

Melting points (compound **2**) were measured using an X-4 melting point apparatus. Mass spectra (MS) and high-resolution mass spectra (HRMS) were recorded using Agilent 6540 Q-Tof (ESIMS) (Agilent, CA, USA). Proton nuclear magnetic resonance (^{1}H-NMR) and carbon-13 NMR (^{13}C-NMR) spectra were recorded using Bruker AVANCE III 500 MHz instruments (Bruker BioSpin GmbH, Rheinstetten, Germany), with tetramethylsilane (TMS) as an internal standard. To perform column chromatography and thin-layer chromatography (TLC), silica gel (200–300 mesh) and silica GF_{254}, respectively, were produced by Qingdao Marine Chemical Company (China).

Recombinant mouse RANKL (R&D Systems, Minneapolis, MN, USA) was reconstituted to a final concentration of 10 μg/mL using sterile phosphate-buffered saline (PBS) containing 0.1% bovine serum albumin (BSA) and then stored at −20 °C. The prepared stock solution was added to the culture medium to achieve the indicated final concentration. Recombinant mouse RANK protein for molecular interaction assay was purchased from R&D Systems. Dulbecco's Modified Eagle's Medium (DMEM) and fetal bovine serum (FBS) were sourced from Hyclone Laboratories (Logan, UT, USA) and Biological Industries (Kibbutz Beit Haemek, Israel), respectively. Mixed penicillin–streptomycin solution (P/S), TRITC-conjugated phalloidin, and antifade mounting medium with DAPI were purchased from Solarbio (Beijing, China). The TRAP staining kit was purchased from Sigma-Aldrich (St. Louis, MO, USA). Specific primary antibodies against NFATc1, c-Src, c-Fos, cathepsin K, and JNK were purchased from Santa Cruz Biotechnology (Santa Cruz, CA, USA). Antibodies against phosphorylated p65 (p-p65), p65, p-JNK, p-ERK1/2, ERK1/2, p-p38, and p38 were purchased from Cell Signaling Technology (Beverly, MA, USA). Anti-TRAP, anti-β-tubulin, and horseradish peroxidase-conjugated secondary antibodies were purchased from Abcam (Cambridge, MA, USA), Proteintech Group, Inc. (IL, USA), and R&D Systems (Minneapolis, MN, USA), respectively.

2.2. Reaction components and extraction

EGCG (0.45 mmol) was maintained in 10 mL of 0.05 M phosphate buffer (Na_2HPO_4, pH 5.8) at 60 °C for 2 h. The reaction mixture was extracted with ethyl acetate (3 × 10 mL), and the combined organic layer was dried over sodium sulfate. The solvent was evaporated under vacuum to obtain the residue.

2.3. HPLC analysis and isolation

Analysis of EGCG and the reaction mixture was performed on an Agilent 1260 LC system, with an XTerra RP-18 (4.6 mm × 250 mm) column. Absorption was detected at 254 nm. The injecting volume was 10 μL, and the flow rate was 1 mL/min. The ratio of mobile phase A (methanol) to phase B (0.5% acetic acid in water) was 20:80. Separation and purification of the compounds were performed on an Agilent 1260 LC system, with an XTerra RP-18 (9.8 mm × 250 mm) column, using 20% methanol solution containing 0.5% acetic acid.

2.4. Characteristics of compound *2*

Compound **2** was a white amorphous powder, m.p. 220–222 °C, ^{1}H-NMR (CD_3OD, 500 MHz) and ^{13}C-NMR (CD_3OD, 125 MHz) data (Table 1); negative-ion ESIMS; *m/z* 457 $[M-H]^-$; negative-ion HRESIMS was calculated for $C_{22}H_{17}O_{11}$ $[M-H]^-$ 457.0849 and was found to be 457.0850.

2.5. Cell culture

Mouse macrophage RAW 264.7 cells obtained from American Type

Table 1
^{1}H-NMR and ^{13}C-NMR data for (-)-gallocatechin gallate (GCG) identified previously and compound **2** identified in this study.

	GCG (δ_1)[a]		Compound **2** (δ_2)	
C position	δ_C	δ_H	δ_C	δ_H
2	77.2	5.52 (d, J = 4.8 Hz)	78.6	5.52 (d, J = 2.4 Hz)
3	69.2	4.96 (dd, J = 4.8 Hz, 10.8 Hz)	69.9	4.96 (d, J = 2.0 Hz)
4	22.6	2.59 (s, H-4α) 2.51 (dd, J = 2.0 Hz, 3.6 Hz, H-4β)	26.8	2.59 (s, H-4α) 2.51 (dd, J = 2.0 Hz, 3.6 Hz, H-4β)
5 (7)	156.5		157.9	
6	95.7	5.93 (d, J = 2.4 Hz)	96.4	5.93 (s)
8	94.3	5.83 (d, J = 2.0 Hz)	95.8	5.93 (s)
9	154.9		157.9	
10	97.5		99.4	
1′	129.0		130.7	
2′, 6′	105.2	6.27 (s)	106.8	6.48 (s)
3′, 5′	146.2		146.7	
4′	132.9		133.8	
1″	119.5		121.4	
2″, 6″	108.9	6.86 (H, s)	110.2	6.93 (s)
3″, 5″	145.8		146.7	
4″	139.0		139.7	
C = O	165.5		167.6	

[a] Experimental data for GCG were obtained from a previous study [27].

Culture Collection (ATCC; TIB-71™; Manassas, VA, USA) were cultured in DMEM supplemented with 10% FBS and 1% P/S. The cells were incubated at 37 °C in a humidified atmosphere of 95% air and 5% CO_2.

2.6. In vitro osteoclastogenesis assay

RANKL induces the differentiation of RAW 264.7 cells into mature osteoclasts *in vitro*, as previously described [21]. To perform the osteoclastogenesis assay, RAW 264.7 cells were seeded in 96-well plates at a density of 1×10^3 cells per well and allowed to adhere overnight. The osteoclast precursor cells were pretreated with or without EGCG (compound **1**, 10 μM) or compound **2** (10 μM) for 20 min in the specific osteoclastogenic medium (DMEM supplemented with 6% FBS and 1% P/S) and subsequently stimulated with RANKL (50 ng/mL) for 4 days. TRAP-positive multinuclear cells were visualized using a TRAP staining kit, according to the manufacturer's instructions. TRAP-positive multinuclear cells with more than three nuclei in each well were counted as mature osteoclasts under a light microscope (Olympus, Tokyo, Japan), and images were acquired with a microscope-aided camera.

2.7. F-actin ring immunofluorescent staining

RAW 264.7 cells (2×10^4 cells per well) were cultured on glass coverslips in a 12-well plate and incubated overnight. The cells were pretreated with or without compound **1** (10 μM) or compound **2** (10 μM) for 20 min in the specific osteoclastogenic medium and subsequently stimulated with RANKL (50 ng/mL) for 6 days. The cells were washed, fixed in 4% paraformaldehyde for 10 min, and permeabilized with 0.1% Triton X-100 for 5 min. Subsequently, the cells were incubated in 150 nM TRITC-conjugated phalloidin at 37 °C for 30 min and then washed with PBS. Finally, the cells were mounted using antifade mounting medium with DAPI for 2 min. F-actin ring distribution was visualized using DM2000 fluorescence microscope (Leica). Images were captured at a magnification of 200X and merged using the ImageJ software (National Institutes of Health, Bethesda, USA).

2.8. RNA extraction and quantitative real-time PCR (qRT-PCR) analysis

RAW 264.7 cells (1×10^5 cells per well) were seeded in 12-well plates and allowed to adhere overnight. Subsequently, RAW 264.7 cells were pretreated with or without compound **1** (10 μM) or compound **2** (10 μM) for 20 min in the specific osteoclastogenic medium and then stimulated with RANKL (50 ng/mL) for 60 h. Then, total RNA was extracted from RAW 264.7 cells using TransZol™ Up Reagent (TransGen Biotech, Beijing, China), according to the manufacturer's protocol. First-strand cDNA was synthesized from the isolated RNA (1 μg) using PrimeScript™ RT Reagent Kit with gDNA Eraser (TaKaRa Bio, Otsu, Japan), according to the manufacturer's instructions. Subsequently, qRT-PCR was performed on a 7900 H T Fast Real-Time PCR system (Applied Biosystems, Foster City, CA, USA) using the TB Green® *Premix Ex Taq*™ II (Tli RNaseH Plus) Reagent (TaKaRa) under the following conditions: 1 cycle of initial denaturation at 95 °C for 30 s, followed by 40 cycles of denaturation at 95 °C for 5 s and annealing and extension at 60 °C for 30 s. Primers used for qRT-PCR were selected from previous studies [21,22] and are listed in Table 2. All reactions were performed in triplicate in a volume of 10 μL. Relative mRNA expression was determined using the comparative $2^{-\Delta\Delta CT}$ method and normalized relative to the *GAPDH* gene (endogenous control).

2.9. Western blot analysis

Cells were washed twice with ice-cold PBS and lysed using RIPA buffer (Solarbio) on ice for protein extraction. The protein lysates were quantified using an Enhanced BCA Protein Assay Kit (Beyotime Biotechnology, Shanghai, China), according to the manufacturer's instructions. To separate the isolated proteins, sodium dodecyl sulfate-polyacrylamide gel electrophoresis (SDS-PAGE) was performed using equal amounts of proteins, which were then transferred to polyvinylidene fluoride (PVDF) membranes (Millipore, Billerica, USA). Proteins of interest were detected by immunoblotting using specific primary antibodies, followed by the corresponding horseradish peroxidase-conjugated secondary antibodies. Hybridization of antibodies to the proteins was detected using an Ultra-sensitive Enhanced Chemiluminescent Substrate Kit (Beijing 4A Biotech Co., Ltd; Beijing, China), and images were captured using a FluorChem E System (ProteinSimple, San Jose, CA, USA). Band densities were quantified using AlphaView software (Cell Biosciences, Santa Clara, CA, USA).

2.10. Molecular interaction assay

Interaction between mouse RANK protein and compound **2** was investigated using biolayer interferometry (BLI) analysis. RANK was biotinylated using amine-PEG3-biotin, as described previously [23]. Then, the reaction mixture was desalted using Zeba Spin desalting columns, and the biotinylated RANK protein was immobilized onto the surface of Super Streptavidin (SSA) biosensors. Increasing concentrations of compound **2** were allowed to interact with the immobilized RANK at 30 °C in PBS (pH 7.4) using an Octet Red 96 instrument (Fortebio, USA). The final volume of all solutions was 200 μL. Assays were performed in black solid 96-well flat bottom plates on a shaker set at 1000 r/min. The association and dissociation of compound **2** with RANK was measured for 600 s each. Kinetic parameters and affinities were calculated from a non-linear global fit of the data between compound **2** and RANK using Octet Data Analysis software version 7.0 (Fortebio).

To test whether compound **2** competes with RANKL to bind to its receptor RANK, a solution competition BLI study was performed using the Octet Red 96 instrument. Briefly, compound **2** (0 or 10 μM) was preincubated with immobilized RANK for 720 s. Then, 0.4 μM RANKL containing 0 or 10 μM compound **2** was allowed to interact with immobilized RANK for 420 s. Finally, dissociation was followed for 420–840 s using 0 or 10 μM compound **2**.

2.11. Statistical analysis

All experimental data were expressed as mean ± standard error of

Table 2
List of primers used for quantitative real-time PCR (qRT-PCR).

Gene	Forward primer (5′→3′)	Reverse primer (5′→3′)
GAPDH	AACTTTGGCATTGTGGAAGG	ACACATTGGGGGTAGGAACA
c-Src	CCAGGCTGAGGAGTGGTACT	CAGCTTGCGGATCTTGTAGT
TRAP	GCTGGAAACCATGATCACCT	GAGTTGCCACACAGCATCAC
cathepsin K	CTTCCAATACGTGCAGCAGA	TCTTCAGGGCTTTCTCGTTC
β3-Integrin	TGACATCGAGCAGGTGAAAG	GAGTAGCAAGGCCAATGAGC
MMP-9	CGTCGTGATCCCCACTTACT	AACACACAGGGTTTGCCTTC
NFATc1	TGGAGAAGCAGAGCACAGAC	GCGGAAAGGTGGTATCTCAA
c-Fos	CAAGCGGAGACAGATCAACTTG	TTTCCTTCTCTTTCAGCAGATTGG

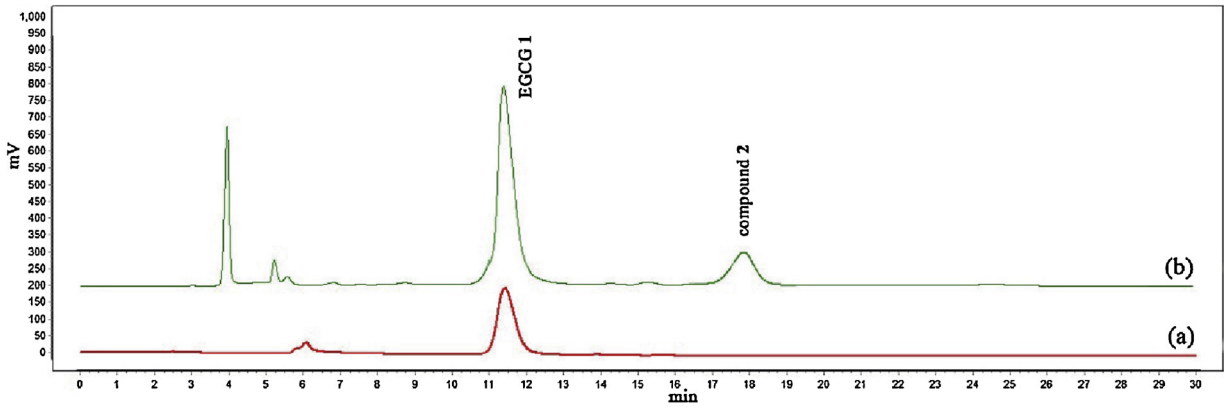

Fig. 1. High performance liquid chromatography (HPLC) analysis of the reaction of (-)-epigallocatechin-3-gallate (EGCG) with phosphate buffer. (**A**) EGCG. (**B**) Reaction of EGCG with 0.5 M phosphate buffer (Na_2HPO_4; pH 5.8) at 60 °C for 2 h.

the mean (SEM) of at least three independent experiments. Statistical analysis was performed using the Student's *t*-test and differences at $P < 0.05$ were considered statistically significant. All analyses were performed using SPSS 17.0 (Chicago, IL, USA) and GraphPad Prism 5 (GraphPad Software, Inc., La Jolla, CA, USA).

3. Results and discussion

3.1. Chemical oxidation and structural determination of EGCG

Chemical oxidation of EGCG has been reported using various oxidative compounds, including $K_3[Fe(CN)_6]$ [24], $CuSO_4$ [25], and $CuCl_2$ [25], that triggered the formation of dimers such as theaflavins, theasinensins, and oolongtheanins and other polymers. Generally, EGCG is oxidized in solution (indicated by changing colors), leading to the formation of an isomer, (-)-gallocatechin gallate (GCG), under acidic catalytic conditions [26,27]. In this study, the chemical oxidation of EGCG was based on the method reported by Xie et al. [27]. EGCG was dissolved in 0.05 M Na_2HPO_4 (pH 5.8) at 60 °C for 2 h, and the mixture was analyzed by HPLC. Interestingly, compound **2** was obtained as the major product on the HPLC spectrum (Fig. 1), with a yield of 60% after extraction and evaporation.

Compound **2** was obtained as a white amorphous powder. One $[M-H]^-$ peak on the MS spectrum demonstrated that the molecular weight of compound **2** was 457, implying that it was an EGCG analogue. On the other hand, in the ^{1}H-NMR spectra (Table 1), the proton at C-2 (5.52 ppm, d, $J = 2.4$ Hz) and C-3 (4.96 ppm, d, $J = 2.0$ Hz) appeared as a double peak, indicating a *cis*-relationship between H-2 and H-3; this product was identified as GCG [27]. The bond between C-2 and O atom was broken under acid catalysis, and the carbon atom at the C-2 position formed tertiary carbocation transition states, generating GCG (Fig. 2).

3.2. Compound 2 is a stronger inhibitor of osteoclast differentiation than EGCG

Numerous studies suggest that tea and its active components, especially catechins, prevent and treat osteoporosis by improving bone mineral density and stimulating osteoblast differentiation, while suppressing osteoclast formation and differentiation [28–30]. EGCG and its derivatives have been reported to exhibit positive effects on bone metabolism [31,32]. However, comparative studies on the anti-osteoclastogenesis activity of EGCG and its oxidation derivative are relatively limited. To investigate whether the inhibitory effect of compound **2** (GCG) on RANKL-induced osteoclast differentiation was comparable with that of EGCG, we treated RAW 264.7 cells with RANKL (50 ng/mL) in the presence of EGCG or compound **2** (10 μM) for 4 days, and TRAP staining was performed to detect osteoclast formation. RAW 264.7 cells differentiated into mature osteoclasts after RANKL stimulation ($P < 0.001$; Fig. 3). When 10 μM of compound **2** was added to the reaction, the RANKL-induced osteoclast formation was almost completely inhibited. However, when EGCG was added to the reaction at the same concentration (10 μM), osteoclast differentiation was only partially inhibited (Fig. 3), which is consistent with the result of a previous study [33]. Compared with EGCG treatment, the number of TRAP-positive multinuclear osteoclast cells decreased significantly following treatment with compound **2** ($P < 0.01$; Fig. 3). These results suggest that compound **2** is a stronger inhibitor of RANKL-induced osteoclast differentiation than EGCG.

3.3. Compound 2 is a stronger inhibitor of RANKL-stimulated F-actin ring formation than EGCG

Mature osteoclasts secrete several proteinases and pump out protons to resorb the bone and form a characteristic actin ring structure to confine the acidic resorbing microenvironment [34]. In this study, mature osteoclasts formed many characteristic circular F-actin rings in the periphery of cells after RANKL stimulation ($P < 0.001$; Fig. 4).

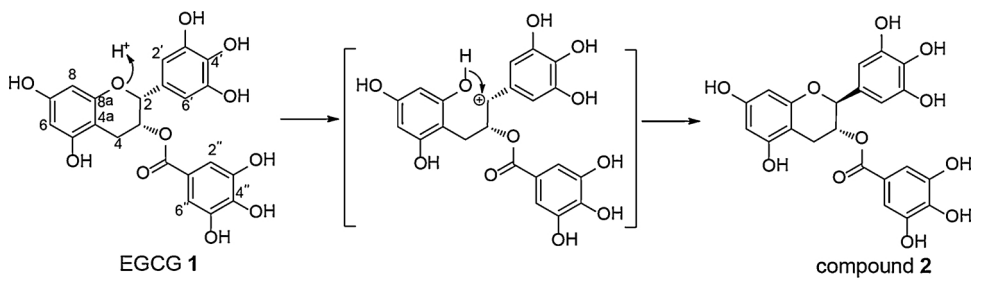

Fig. 2. Schematic representation of a plausible mechanism for the conversion of EGCG to GCG.

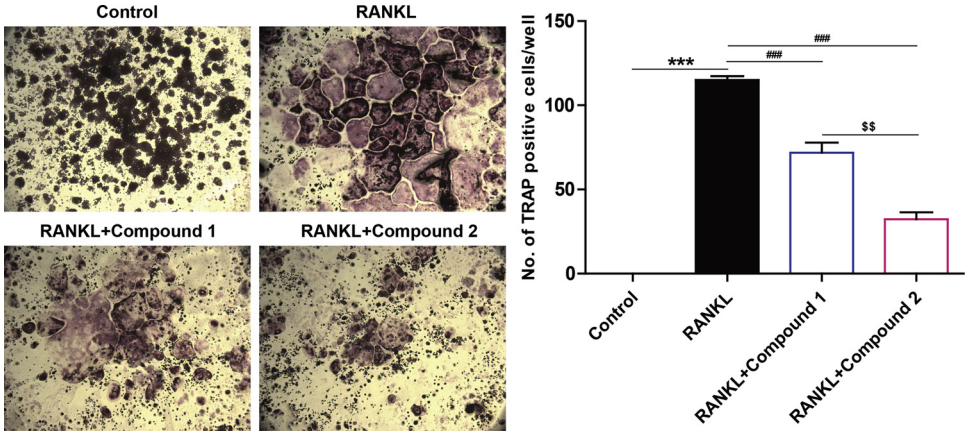

Fig. 3. Compound **2** inhibits osteoclast differentiation more effectively than EGCG. RAW 264.7 cells were pretreated with or without compound **1** (EGCG, 10 μM) or compound **2** (10 μM) for 20 min in an osteoclastogenic medium and subsequently stimulated with RANKL (50 ng/mL) for 4 days. Cells were stained with TRAP; TRAP-positive multinuclear cells with more than three nuclei in each well were counted under a microscope (original magnification 40X). Representative images are shown. Data represent mean ± standard error of mean (SEM) of three independent replicates. $^{***}P < 0.001$ compared with the control; $^{\#\#\#}P < 0.001$ compared with RANKL treatment only; $^{\$\$}P < 0.01$ compared with compound **1** treatment.

However, treatment with EGCG or compound **2** significantly suppressed the formation of F-actin rings ($P < 0.001$). Unsurprisingly, compound **2** inhibited RANKL-stimulated F-actin ring formation more strongly than EGCG ($P < 0.01$).

3.4. Compound 2 significantly inhibits the expression of osteoclastogenesis-related marker genes and proteins more than EGCG

Osteoclast differentiation and activation are executed directly by the expression of a large number of marker genes, such as c-Src, TRAP, cathepsin K, β3-Integrin, and MMP-9 [8,21]. To further confirm that compound **2** inhibits RANKL-induced osteoclastogenesis more effectively than EGCG, we examined the expression of osteoclastogenesis-specific marker genes and proteins after treatment with EGCG or compound **2**. The results of qRT-PCR analysis demonstrated that the mRNA expression levels of c-Src, TRAP, cathepsin K, β3-Integrin, and MMP-9 were significantly increased by the stimulation of RANKL ($P < 0.001$; Fig. 5A–E) but significantly down-regulated after treatment with EGCG or compound **2** ($P < 0.01$). Compared with EGCG treatment, the expression of these osteoclastogenesis-specific marker genes significantly decreased following compound **2** treatment ($P < 0.001$). Additionally, EGCG or compound **2** significantly suppressed the expression of osteoclast-related marker proteins, including c-Src, TRAP, and cathepsin K ($P < 0.01$; Fig. 5F–I). Furthermore, compound **2** inhibited the protein expression of c-Src and TRAP significantly more effectively than EGCG ($P < 0.001$; Fig. 5F–H), which was consistent with the results of qRT-PCR analysis.

3.5. Compound 2 significantly suppresses RANKL-induced expression of NFATc1 and c-Fos more than EGCG

Many transcription factors are essential for promoting osteoclast-related gene expression during osteoclastogenesis [8,9]. To understand the inhibitory mode of action of compound **2** on RANKL-induced osteoclast differentiation, the expression of NFATc1 and c-Fos, master transcriptional regulators of osteoclastogenesis [34], were examined using qRT-PCR and western blotting analysis. The results showed that mRNA and protein expression levels of NFATc1 and c-Fos were significantly increased by the stimulation of RANKL ($P < 0.001$; Fig. 6) but significantly decreased following treatment with EGCG or compound **2** ($P < 0.05$). In addition, compound **2** significantly suppressed the expression of these key transcription factors more than EGCG ($P < 0.05$; Fig. 6). On the basis of these results, we confirmed the inhibitory effect of the EGCG oxidation derivative (compound **2**) on RANKL-induced osteoclastogenesis in RAW 264.7 cells.

3.6. Compound 2 inhibits RANKL-induced phosphorylation of p65 and MAPK in RAW 264.7 cells

To further illuminate the molecular mechanisms underlying the

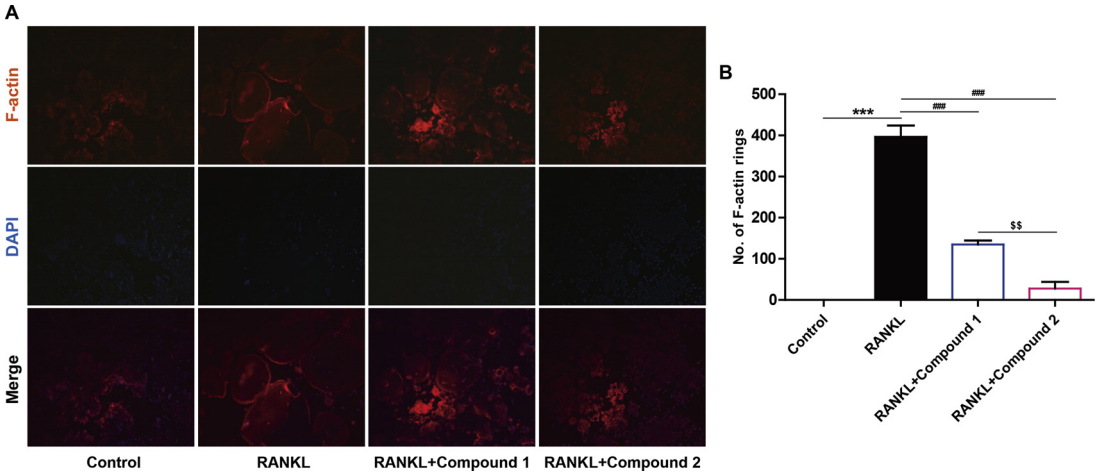

Fig. 4. Compound **2** inhibits RANKL-stimulated F-actin ring formation more strongly than EGCG. RAW 264.7 cells were pretreated with or without compound **1** (EGCG, 10 μM) or compound **2** (10 μM) for 20 min in an osteoclastogenic medium and subsequently stimulated with RANKL (50 ng/mL) for 6 days. F-actin rings and nuclei were stained with TRITC-conjugated phalloidin and DAPI, respectively. Representative images are displayed (original magnification 200X); images were merged using the ImageJ software. Data represent mean ± SEM of three independent replicates. $^{***}P < 0.001$ compared with the control; $^{\#\#\#}P < 0.001$ compared with RANKL treatment only; $^{\$\$}P < 0.01$ compared with compound **1** treatment.

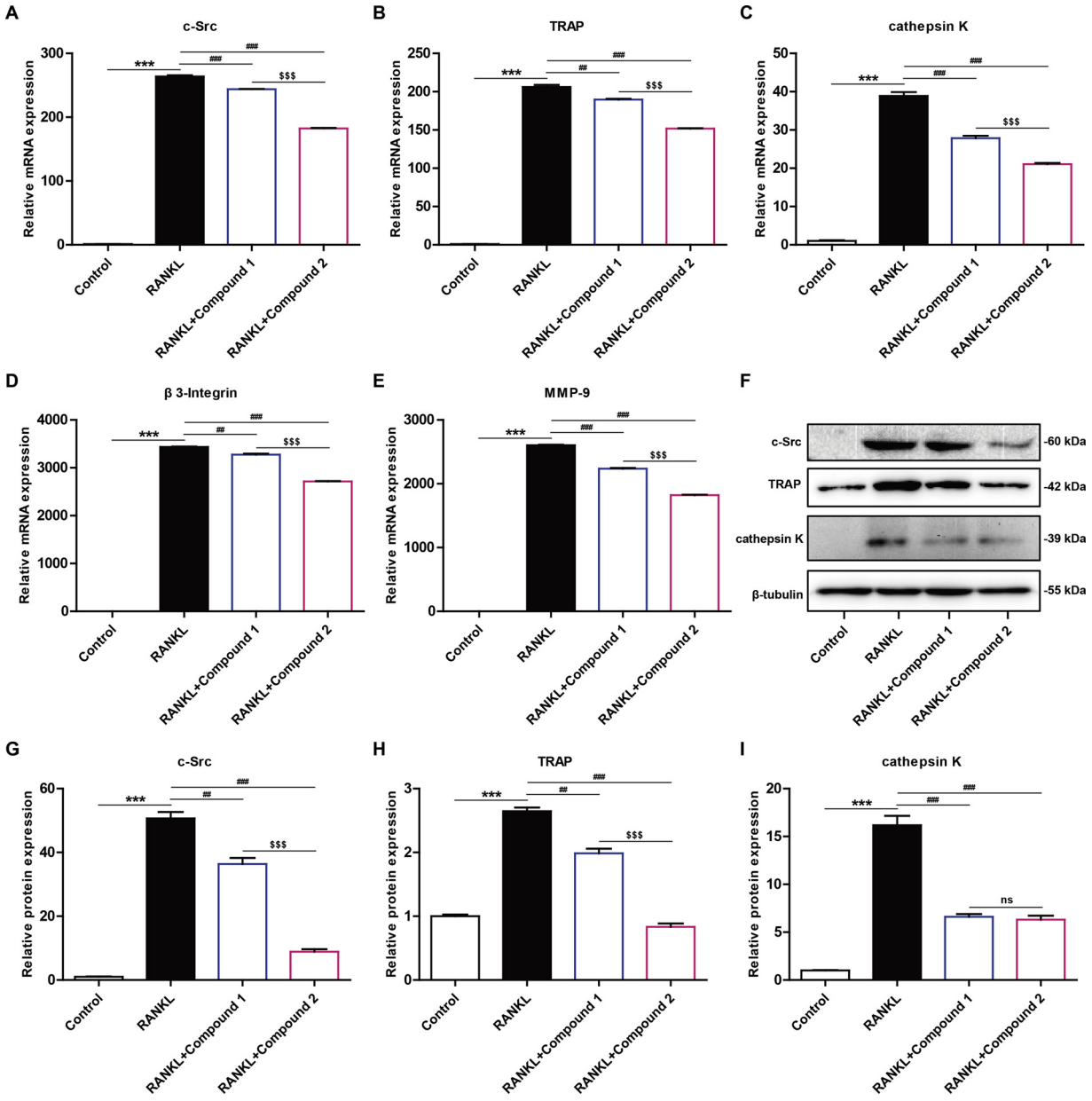

Fig. 5. Compound **2** significantly inhibits the expression of osteoclastogenesis-related marker genes and proteins more than EGCG. RAW 264.7 cells were pretreated with or without compound **1** (EGCG, 10 μM) or compound **2** (10 μM) for 20 min in an osteoclastogenic medium and subsequently stimulated with RANKL (50 ng/mL) for 60 h. (**A–E**) Analysis of c-Src (**A**), TRAP (**B**), cathepsin K (**C**), β3-Integrin (**D**), and MMP-9 (**E**) genes by qRT-PCR. (**F**) Western blotting analysis of c-Src, TRAP, and cathepsin K proteins. Representative images are shown. (**G–I**) Gray densities of bands corresponding to c-Src (**G**), TRAP (**H**), and cathepsin K (**I**) quantified using AlphaView software. Data represent mean ± SEM of three independent replicates. $^{***}P < 0.001$ compared with the control; $^{\#\#}P < 0.01$ and $^{\#\#\#}P < 0.001$ compared with RANKL treatment only; $^{\$\$\$}P < 0.001$ compared with compound **1** treatment. ns, not significant.

inhibitory effects of compound **2** on RANKL-induced osteoclastogenesis and NFATc1 and c-Fos expression, we examined the effects of compound **2** on RANKL-induced early canonical RANK signaling pathways, including NF-κB and MAPK (JNK, ERK, and p38), which activate key transcription factors such as NFATc1 and c-Fos during osteoclastogenesis [8,9]. Phosphorylation of these signaling molecules was observed in RAW 264.7 cells at 5 min after RANKL treatment (Fig. 7A). Within 60 min of stimulation with RANKL, phosphorylation of p65 ($P < 0.01$; Fig. 7B), JNK ($P < 0.01$; Fig. 7C), ERK1/2 ($P < 0.01$; Fig. 7D), and p38 ($P < 0.05$; Fig. 7E) relative to total p65, total JNK, total ERK1/2, and total p38 were significantly suppressed by compound **2** treatment in RAW 264.7 cells. Collectively, these results indicate that compound **2** exerts an inhibitory effect on RANKL-stimulated NF-κB and MAPK activation pathways.

*3.7. Compound **2** binds to RANK with high affinity and blocks RANKL–RANK interactions*

Protein–protein interactions between RANKL and RANK are known to manipulate the differentiation and activation of osteoclasts during bone remodeling and are therefore considered a pivotal therapeutic target for the treatment of osteoporosis [35]. Given the inhibitory effects of compound **2** on RANKL-induced early RANK signaling pathways including p65, JNK, ERK, and p38, we further examined whether compound **2** blocks RANKL–RANK interactions. First, the binding affinity of compound **2** for RANK was detected using BLI analysis (Fig. 8A). The results showed that compound **2** directly interacts with RANK. The apparent association (K_{on}) and dissociation (K_{off}) constants of compound **2** were estimated as 2.27×10^2 $M^{-1}s^{-1}$ and 4.28×10^{-5} s^{-1},

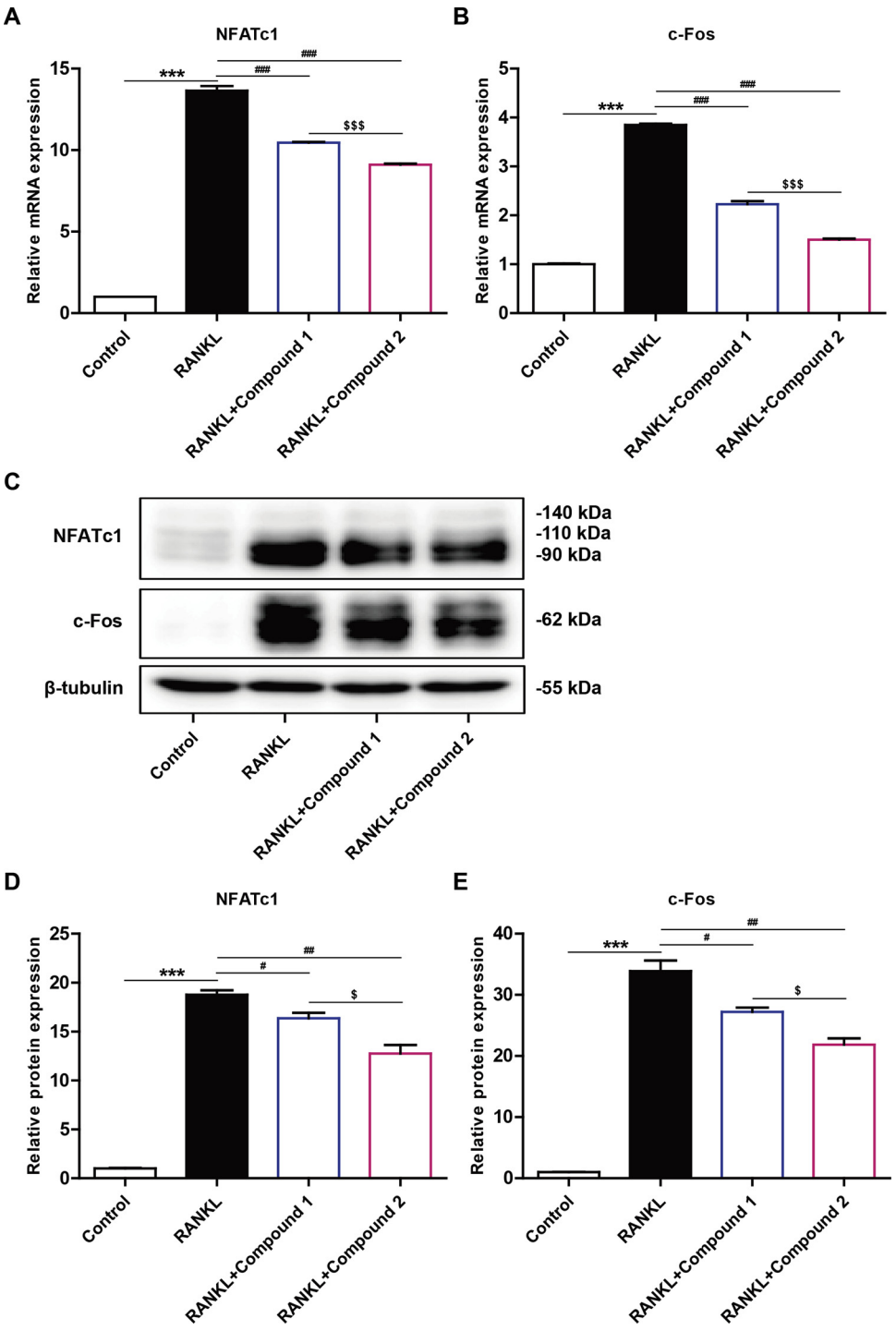

Fig. 6. Compound **2** significantly suppresses RANKL-induced expression of NFATc1 and c-Fos more than EGCG. Treatment conditions were the same as described in Fig. 5. (**A, B**) Expression analysis of NFATc1 (**A**) and c-Fos (**B**) by qRT-PCR. (**C**) Western blotting analysis of NFATc1 and c-Fos proteins. Representative images are shown. (**D, E**) Gray densities of bands corresponding to NFATc1 (**D**) and c-Fos (**E**) quantified using AlphaView software. Data represent mean ± SEM of three independent replicates. $^{***}P < 0.001$ compared with the control; $^{\#}P < 0.05$, $^{\#\#}P < 0.01$, and $^{\#\#\#}P < 0.001$ compared with RANKL treatment only; $^{\$}P < 0.05$ and $^{\$\$\$}P < 0.001$ compared with compound **1** treatment.

respectively, and RANK-binding affinity (K_D) was estimated as 189 nM (Fig. 8A). These data suggest that the RANK–compound **2** complex is relatively stable. Next, solution competition BLI assay revealed that compound **2** has the ability to compete with RANKL to bind to its receptor RANK (Fig. 8B), suggesting that compound **2** blocks RANKL–-RANK interactions. These results suggest the receptor RANK as a potential direct interaction target of compound **2** in the inhibition of osteoclastogenesis, although this needs further verification in the future.

To maintain bone homeostasis, a balance must be achieved between bone resorption and bone formation [1]. Tea catechin EGCG has been shown to enhance osteoblast differentiation [36]. However, whether the oxidation derivative of EGCG, compound **2,** could stimulate osteoblast differentiation needs further investigation. Additionally, there is an urgent need to investigate the potential anti-osteoporosis effects of compound **2** *in vivo*.

4. Conclusion

In this study, we demonstrated for the first time that an EGCG oxidation derivative (compound **2**) inhibits RANKL-induced osteoclastogenesis and F-actin ring formation more effectively than EGCG through the down-regulation of NFATc1 and c-Fos. Compound **2** showed binding to RANK with high affinity (K_D = 189 nM) and blocked RANKL–RANK interactions, thereby suppressing RANKL-induced early RANK signaling pathways including p65, JNK, ERK, and p38 in

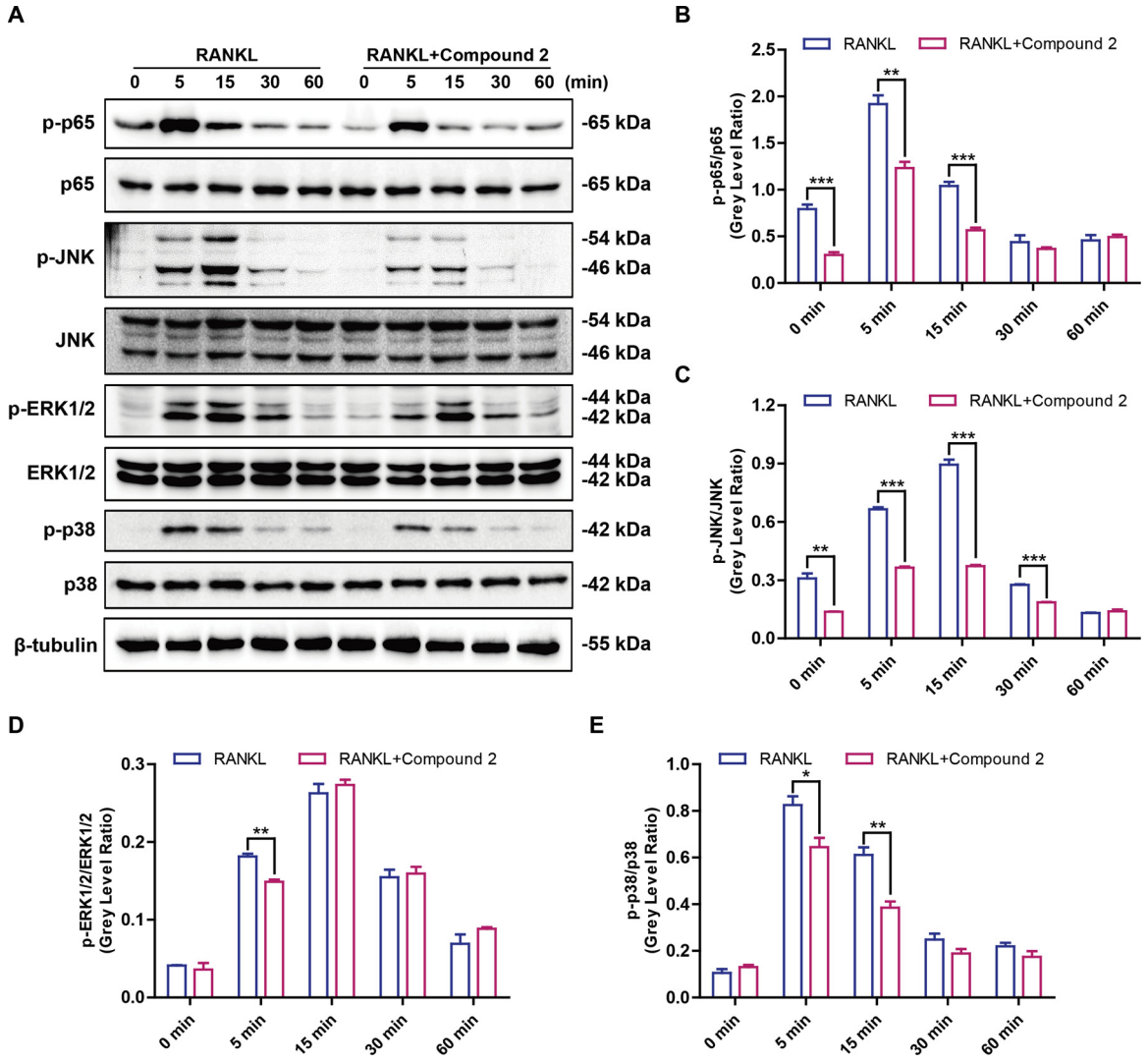

Fig. 7. Compound **2** suppresses RANKL-stimulated phosphorylation of p65 and MAPK. (**A**) RAW 264.7 cells were pretreated with or without compound **2** (10 μM) for 3 h in serum-free medium and then stimulated with RANKL (50 ng/mL) for the indicated times. Cell lysates were subjected to western blotting using the indicated primary antibodies. Representative images are shown. (**B–E**) Quantification of the ratios of band intensity relative to total p65 (**B**), total JNK (**C**), total ERK1/2 (**D**), and total p38 (**E**). Data are expressed as mean ± SEM of three independent experiments. Asterisks indicate significant differences compared with the RANKL treatment at the same time point ($^{*}P < 0.05$; $^{**}P < 0.01$; $^{***}P < 0.001$).

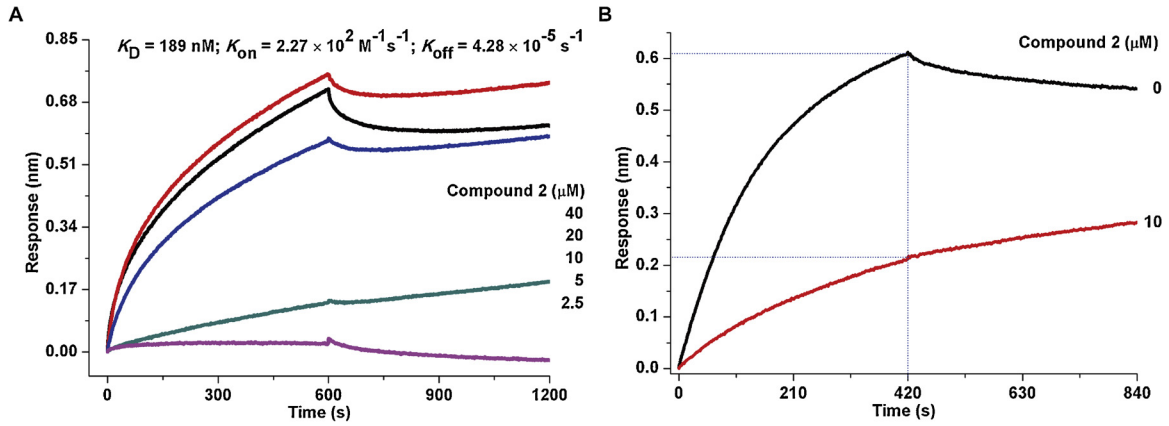

Fig. 8. Compound **2** binds to RANK with high affinity and blocks RANKL–RANK interactions. (**A**) BLI sensorgrams indicating the interactions between gradient concentrations of compound **2** and RANK were measured on an Octet Red 96 system, with association and dissociation for 600 s each. These sensorgrams were used to determine the binding affinity (K_D), association constant (K_{on}), and dissociation constant (K_{off}). (**B**) Compound **2** competes with RANKL to bind to its receptor RANK in the solution competition BLI assay. Compound **2** (0 or 10 μM) was preincubated with 0.4 μM RANKL prior to interaction with immobilized RANK. Sensorgrams correspond to the phases of association and dissociation for 420 s each.

osteoclast precursors.

Author contributions

Jun Sheng, Xuanjun Wang, Huanhuan Xu, and Chengting Zi conceived and designed the experiments. Huanhuan Xu, Titi Liu, Jin Li, Jing Xu, Chengting Zi, Fei Chen, Lihong Hu, and Banglei Zhang performed the experiments. Huanhuan Xu and Chengting Zi analyzed the data. Jun Sheng and Xuanjun Wang contributed reagents/materials/analysis tools. Huanhuan Xu, Titi Liu, and Chengting Zi wrote the manuscript. Huanhuan Xu, Titi Liu, and Jin Li revised the manuscript. All authors read and approved the final version manuscript.

Funding

This study was supported in part by research grants from the Scholarship for Academic Leader of Yunnan Province (2017HA015), the Major Scientific and Technological Special Project of Yunnan Province (2017ZF003, 2018ZG010 and 2018ZG013), the National Natural Science Foundation of China (21602196), and the National Natural Science Foundation of Yunnan Province (2017FD084). The funders had no role in the study design, data collection and analysis, decision to publish, or preparation of the manuscript.

Declaration of Competing Interest

The authors declare no conflict of interest.

References

[1] W.J. Boyle, W.S. Simonet, D.L. Lacey, Osteoclast differentiation and activation, Nature 423 (6937) (2003) 337–342.
[2] B. Kim, K.Y. Lee, B. Park, Icariin abrogates osteoclast formation through the regulation of the RANKL-mediated TRAF6/NF-kappaB/ERK signaling pathway in Raw264.7 cells, Phytomedicine 51 (2018) 181–190.
[3] T. Negishi-Koga, H. Takayanagi, Ca2+-NFATc1 signaling is an essential axis of osteoclast differentiation, Immunol. Rev. 231 (1) (2009) 241–256.
[4] B. Langdahl, S. Ferrari, D.W. Dempster, Bone modeling and remodeling: potential as therapeutic targets for the treatment of osteoporosis, Ther. Adv. Musculoskelet. Dis. 8 (6) (2016) 225–235.
[5] T. Liu, Z. Xiang, F. Chen, D. Yin, Y. Huang, J. Xu, L. Hu, H. Xu, X. Wang, J. Sheng, Theabrownin suppresses in vitro osteoclastogenesis and prevents bone loss in ovariectomized rats, Biomed. Pharmacother. 106 (2018) 1339–1347.
[6] L. Zhou, Q. Liu, G. Hong, F. Song, J. Zhao, J. Yuan, J. Xu, R.X. Tan, J. Tickner, Q. Gu, Cumambrin A prevents OVX-induced osteoporosis via the inhibition of osteoclastogenesis, bone resorption, and RANKL signaling pathways, FASEB J 33 (6) (2019) 6726–6735.
[7] V. Nagy, J.M. Penninger, The RANKL-RANK story, Gerontology 61 (6) (2015) 534–542.
[8] K. Chen, P. Qiu, Y. Yuan, L. Zheng, J. He, C. Wang, Q. Guo, J. Kenny, Q. Liu, J. Zhao, J. Chen, J. Tickner, S. Fan, X. Lin, J. Xu, Pseurotin a inhibits osteoclastogenesis and prevents ovariectomized-induced bone loss by suppressing reactive oxygen species, Theranostics 9 (6) (2019) 1634–1650.
[9] K. Zhao, Y. Jia, J. Peng, C. Pang, T. Zhang, W. Han, J. Jiang, X. Lu, J. Zhu, Y. Qian, Anacardic acid inhibits RANKL-induced osteoclastogenesis in vitro and prevents ovariectomy-induced bone loss in vivo, FASEB J. 33 (8) (2019) 9100–9115.
[10] Z.M. Chen, Z. Lin, Tea and human health: biomedical functions of tea active components and current issues, J. Zhejiang Univ. Sci. B 16 (2) (2015) 87–102.
[11] H. Xu, T. Liu, L. Hu, J. Li, C. Gan, J. Xu, F. Chen, Z. Xiang, X. Wang, J. Sheng, Effect of caffeine on ovariectomy-induced osteoporosis in rats, Biomed. Pharmacother. 112 (2019) 108650.
[12] L.A. Nash, W.E. Ward, Tea and bone health: findings from human studies, potential mechanisms, and identification of knowledge gaps, Crit. Rev. Food Sci. Nutr. 57 (8) (2017) 1603–1617.
[13] N. Khan, H. Mukhtar, Tea polyphenols in promotion of human health, Nutrients 11 (1) (2018).
[14] J. Xu, Z. Xu, W. Zheng, A review of the antiviral role of green tea catechins, Molecules 22 (8) (2017).
[15] A. Negri, V. Naponelli, F. Rizzi, S. Bettuzzi, Molecular targets of epigallocatechin-gallate (EGCG): a special focus on signal transduction and cancer, Nutrients 10 (12) (2018).
[16] T. Wang, Z. Xiang, Y. Wang, X. Li, C. Fang, S. Song, C. Li, H. Yu, H. Wang, L. Yan, S. Hao, X. Wang, J. Sheng, (-)-Epigallocatechin gallate targets notch to attenuate the inflammatory response in the immediate early stage in human macrophages, Front. Immunol. 8 (2017) 433.
[17] S.T. Chen, L. Kang, C.Z. Wang, P.J. Huang, H.T. Huang, S.Y. Lin, S.H. Chou, C.C. Lu, P.C. Shen, Y.S. Lin, C.H. Chen, (-)-Epigallocatechin-3-Gallate Decreases Osteoclastogenesis via Modulation of RANKL and Osteoprotegrin, Molecules 24 (1) (2019).
[18] S.H. Lee, B.J. Kim, H.J. Choi, S.W. Cho, C.S. Shin, S.Y. Park, Y.S. Lee, S.Y. Lee, H.H. Kim, G.S. Kim, J.M. Koh, (-)-Epigallocathechin-3-gallate, an AMPK activator, decreases ovariectomy-induced bone loss by suppression of bone resorption, Calcif. Tissue Int. 90 (5) (2012) 404–410.
[19] M. Friedman, H.S. Jurgens, Effect of pH on the stability of plant phenolic compounds, J. Agric. Food Chem. 48 (6) (2000) 2101–2110.
[20] J. Wang, H. Tang, B. Hou, P. Zhang, J. Sheng, Synthesis, antioxidant activity, and density functional theory study of catechin derivatives, RSC Adv. 7 (85) (2017) 54136–54141.
[21] H. Xu, D. Yin, T. Liu, F. Chen, Y. Chen, X. Wang, J. Sheng, Tea polysaccharide inhibits RANKL-induced osteoclastogenesis in RAW264.7 cells and ameliorates ovariectomy-induced osteoporosis in rats, Biomed. Pharmacother. 102 (2018) 539–548.
[22] T. Liu, S. Ding, D. Yin, X. Cuan, C. Xie, H. Xu, X. Wang, J. Sheng, Pu-erh tea extract ameliorates ovariectomy-induced osteoporosis in rats and suppresses osteoclastogenesis in vitro, Front. Pharmacol. 8 (2017) 324.
[23] H. Xu, Y. Wang, Y. Chen, P. Zhang, Y. Zhao, Y. Huang, X. Wang, J. Sheng, Subcellular localization of galloylated catechins in tea plants [*Camellia sinensis* (L.) O. Kuntze] assessed via immunohistochemistry, Front. Plant Sci. 7 (2016) 728.
[24] Y. Takino, H. Imagawa, Y. Aoki, T. Ozawa, Studies on the mechanism of the oxidation of tea leaf catechins, Agric. Chem. Soc. Jpn. J. 45 (8) (1971) 176–183.
[25] S. Takuya, M. Makoto, M. Yosuke, T. Takashi, K. Isao, Biomimetic one-pot preparation of a black tea polyphenol theasinensin A from epigallocatechin gallate by treatment with copper(II) chloride and ascorbic acid, Chem. Pharm. Bull. 59 (9) (2011) 1183–1185.
[26] T. Hatano, M. Hori, M. Kusuda, T. Ohyabu, H. Ito, T. Yoshida, Characterization of the oxidation products of (-)-epigallocatechin gallate, a bioactive tea polyphenol, on incubation in neutral solution, Heterocycles 63 (2004) 1547–1554.
[27] L. Xie, Y. Guo, C. Bo, Y. Jing, Epimerization of epigallocatechin gallate to gallocatechin gallate and its anti-diabetic activity, Med. Chem. Res. 22 (7) (2013) 3372–3378.
[28] C.L. Shen, J.K. Yeh, J.J. Cao, J.S. Wang, Green tea and bone metabolism, Nutr. Res. 29 (7) (2009) 437–456.
[29] Y. Oka, S. Iwai, H. Amano, Y. Irie, K. Yatomi, K. Ryu, S. Yamada, K. Inagaki, K. Oguchi, Tea polyphenols inhibit rat osteoclast formation and differentiation, J. Pharmacol. Sci. 118 (1) (2012) 55–64.
[30] C.H. Ko, K.M. Lau, W.Y. Choy, P.C. Leung, Effects of tea catechins, epigallocatechin, gallocatechin, and gallocatechin gallate, on bone metabolism, J. Agric. Food Chem. 57 (16) (2009) 7293–7297.
[31] J. Xi, Q. Li, X. Luo, J. Li, L. Guo, H. Xue, G. Wu, Epigallocatechin3gallate protects against secondary osteoporosis in a mouse model via the Wnt/betacatenin signaling pathway, Mol. Med. Rep. 18 (5) (2018) 4555–4562.
[32] T. Tominari, R. Ichimaru, S. Yoshinouchi, C. Matsumoto, K. Watanabe, M. Hirata, F.M.W. Grundler, M. Inada, C. Miyaura, Effects of O-methylated (-)-epigallocatechin gallate (EGCG) on LPS-induced osteoclastogenesis, bone resorption, and alveolar bone loss in mice, FEBS Open Bio 7 (12) (2017) 1972–1981.
[33] J.H. Lee, H. Jin, H.E. Shim, H.N. Kim, H. Ha, Z.H. Lee, Epigallocatechin-3-gallate inhibits osteoclastogenesis by down-regulating c-Fos expression and suppressing the nuclear factor-kappaB signal, Mol. Pharmacol. 77 (1) (2010) 17–25.
[34] K. Kim, T.H. Kim, H.J. Ihn, J.E. Kim, J.Y. Choi, H.I. Shin, E.K. Park, Inhibitory effect of purpurogallin on osteoclast differentiation in vitro through the downregulation of c-Fos and NFATc1, Int. J. Mol. Sci. 19 (2) (2018).
[35] C. Liu, X. Chen, X. Zhi, W. Weng, Q. Li, X. Li, Y. Zou, J. Su, H.G. Hu, Structure-based development of an osteoprotegerin-like glycopeptide that blocks RANKL/RANK interactions and reduces ovariectomy-induced bone loss in mice, Eur. J. Med. Chem. 145 (2018) 661–672.
[36] S.Y. Lin, L. Kang, C.Z. Wang, H.H. Huang, T.L. Cheng, H.T. Huang, M.J. Lee, Y.S. Lin, M.L. Ho, G.J. Wang, C.H. Chen, (-)-Epigallocatechin-3-gallate (EGCG) enhances osteogenic differentiation of human bone marrow mesenchymal stem cells, Molecules 23 (12) (2018).